SECTORIAL-EXPANSION ANALYSIS OF IRREGULARLY COILED SHELLS; APPLICATION TO THE RECENT GASTROPOD *DISTORSIO*

by ANTONIO CHECA *and* ROQUE AGUADO

ABSTRACT. In a sectorial-expansion analysis the shell can be described as a series of independent helicospirals joining homologous points on the shell's surface. In actual shells, these helicospirals are longitudinal ornaments. Therefore, the aperture is considered as a set of points, obtained at its intersection with these ornaments. Any apertural segment (between two consecutive points) is potentially able to expand or contract independently during growth. With the aim of quantifying this change in length in any coiled shell, a differential parameter (S_c) has been devised. S_c measures the rate at which any apertural chord of length D varies with regard to a particular spiral length (L_m). This morphometric analysis has been performed on the gastropod *Distorsio reticulata*. The ontogenetic distribution of S leads us to conclude that the distorted, periodically bulging spiral of this species is constructed by alternatively expanding and contracting the apertural mantle. This striking morphology might allow the animal to retract the body deeply within the shell as a passive defence and improves its stability on the substrate.

THE existing methods of theoretical shell morphology imply major differences in the principles that generate shell morphologies (for a general survey see Savazzi 1990). We will briefly comment on two alternative ways of considering the shell. In the tube models, shells are obtained by the motion of a generating curve along a trajectory. This trajectory may define the equiangular spiral (Raup 1961, 1962, 1966, 1967; Raup and Michelson 1965), or be given by more complicated differential equations (Okamoto 1988*a*, 1988*b*, 1988*c*; Ackerly 1989*a*, 1989*b*; Illert 1989). A limitation of these models is that cross-sections and apertures, usually circular, either remain geometrically similar throughout ontogeny or change according to simple allometric laws. On the other hand, in the models of McGhee (1978, 1980*a*, 1980*b*) and Savazzi (1985*a*, 1985*b*, 1987) the shell is described as a set of independent helicospirals and the aperture at each growth stage is obtained by joining the corresponding points of adjacent helicospirals. Since these models are based on Raup's equiangular spiral, they do not cover the whole spectrum of shell morphologies (in contrast to the moving reference frame models of Okamoto, Ackerly and Illert), although aperture shape can be made to vary in many ways by allowing the different helicospirals to differ in their parameters.

In the sectorial-expansion analysis of Checa (1991) the second alternative was followed, but each helicospiral, rather than being a theoretical line, links homologous points on the shell surface. In actual shells, sequences of homologous points are longitudinal ornaments (mainly ribs and striations). When meeting the cross-section or aperture, the helicospirals bound sectors which may evolve independently one from another. On this basis a parameter was devised (the sectorial-expansion rate) to estimate the rate (per radian) at which a cross-sectional sector expands or contracts in helically coiled shells. Although coiling was not directly described by this analysis, the sectorial-expansion rate provided useful information about small-scale changes taking place at the shell edge. The main objective of this morphometric analysis was the study of the biological generating curve, while earlier theoretical models concentrated mainly on the theoretical generating curve.

Since Checa's (1991) sectorial-expansion rate derives from Raup's model, its measurement is restricted to cross-sections of shells coiling around a single axis. Therefore, defining another

[Palaeontology, Vol. 35, Part 4, 1992, pp. 913–925.]

sectorial-expansion rate obtainable at the aperture of any shell morphology is of great interest within this research programme. The present study is mainly concerned with obtaining such a parameter and checking what information it can provide about shell morphology and morphogenesis. There is a priori one limitation inherent in this methodology: it is restricted to shells displaying sequences of homologous points on their external or internal surfaces, and the only features recognizable as such are longitudinal ornaments (sculpture and colour bands). This identity is the base of some morphogenetic studies at the cellular level (see e.g. Meinhardt 1984; Meinhardt and Klinger 1987).

CALCULATION OF THE SECTORIAL-EXPANSION RATE

Geometrical principles

A sectorial-expansion rate is conceived as the rate at which a given apertural or cross-sectional sector chord length (D) varies with respect to another shell parameter. To allow sectors of the same or different shells to be compared, this rate must be standardized. Sector area is also a suitable parameter, but its calculation and standardization are more difficult and the result is no more informative than D.

The first question to be asked is: with respect to which parameter must D be calculated? If the resulting rate is to be of general applicability, the revolution angle can be excluded, because many shells do not coil according to the equiangular spiral or do not coil at all. Another potential parameter is the total length of the shell or growth stage, but this would require a knowledge of the exact function associated with, for instance, the shell's centre of gravity, which would make the procedure impractical.

We will apply another principle. The shell is seen as a succession of growth increments of infinitesimal thickness, and only the growth direction at each point of the aperture is taken into account. The growth direction can be represented by a vector originating at the point and coinciding with the tangent to the corresponding trajectory of homologous points (a similar vectorial approach can be found in Seed 1980, fig. 8). Each sector is then bounded by two such vectors. Additionally, a triangle is formed by the intersection of the aperture and both tangents (Text-fig. 1). In general these tangents will be non-coplanar, so what we actually do is project them onto an intermediate plane.

In very particular cases, the distances at which these tangents intersect (L_1 and L_2 in Text-fig. 1) are equivalent to the distances at which the respective trajectories intersect (provided that a helicospiral can be locally adjusted to these trajectories). This is true when both trajectories coil around the revolution surface of a straight line (cone or cylinder), provided that the tangents are traced at the same coiling angle. This can be demonstrated by a simple experiment (Text-fig. 2): the ends of two wires are attached at two points aligned in parallel to the axis of a cylinder, around which the wires are wound in such a way that they meet towards the centre. The tangents to the wires (and hence to the functions they describe) are the straight traces left by the wires when the cylinder rolls on a planar surface. It is thus evident that the tangents will intersect at the same distances as do the wound wires. The same applies to two wires wound around a cone, that is, logarithmic helicospirals. In both cases the local functions followed by the homologous-point successions at the shell aperture may be substituted by their tangents. This is not commonly the case, since most trajectories in actual shells coil around different cones.

A certain analogy can be established between our methodology and finite-element analysis, in which a three-dimensional figure is converted into many planar polygons (usually triangles). Actual shapes are better approximated by increasing the number of triangles. In our case, reducing the relative size of D leads to the same effect.

Sectorial-expansion rate S′

The triangle depicted in Text-figure 1 has three sides, two of which (L_1 and L_2) have already been defined. The third (D) is the chord of the arc. From this construction we may obtain the expansion

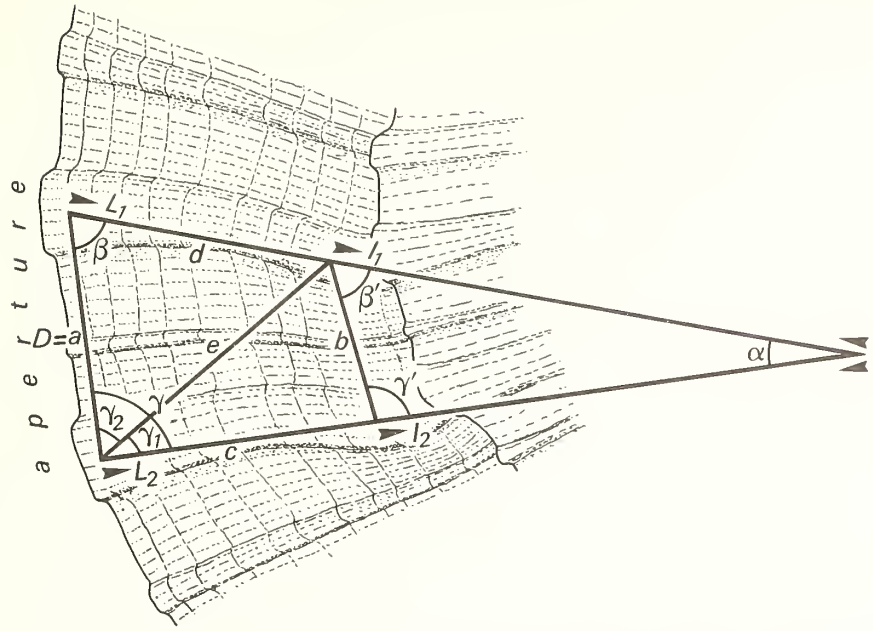

TEXT-FIG. 1. Triangular arrangement between two series of homologous points (ribs) at the apertural flaring of *Distorsio reticulata* Röding (MNCN.P-M-4.317*a*). For symbols see text. Camera lucida drawing.

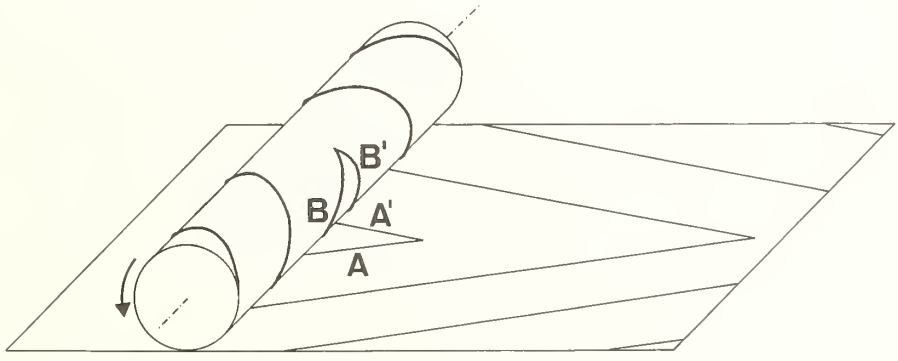

TEXT-FIG. 2. The wound wires experiment: two wires are wound around a cylinder so that they meet at a given central point. Straight traces left by the wires (previously impregnated with ink) when the cylinder rolls on a white paper sheet are the tangents to the wires. It is clear that these tangents intersect at the same distances (A and A′) as the two wires (B and B′).

rate of D provided that we find an adequate parameter with respect to which we can calculate the derivative of D. The best choice seems to be a combination of the lengths of both L_1 and L_2, for D increases linearly with either of them. The simple average of L_1 and L_2 is not representative of the average trajectory length; we simply have to think of an isosceles triangle, in which L_1 and L_2 are always longer than any other straight trajectory lying between them. It will be better to consider the mean length (L_m) of the array of lines extending from the intersection of L_1 and L_2 to D (Text-fig. 3A), since D/L_m in any triangle is the single sum of the many $(D/L_m)_i$ obtained when the triangle is partitioned into n portions of α (i varying from 1 to n), so that the additive property is kept.

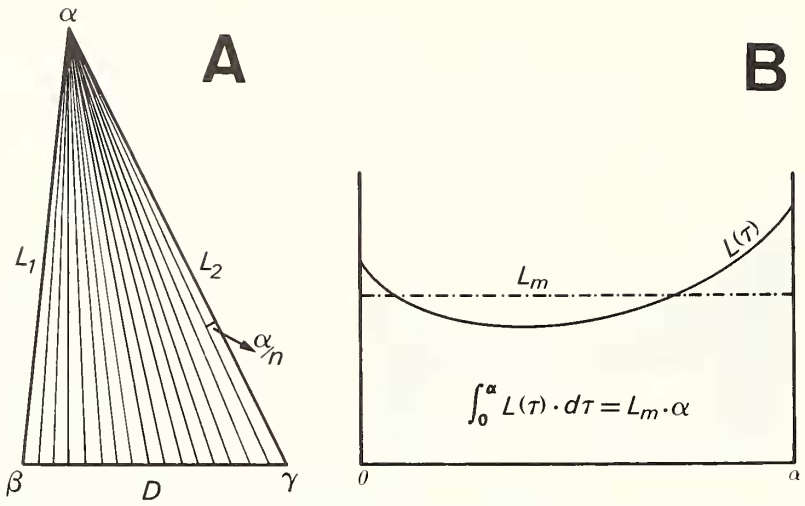

TEXT-FIG. 3. Determination of L_m. A, an array of lines with different lengths (L) are traced from the vertex of angle α to D, taking an α/n constant step. B, L defines a function $L(\tau)$, τ being the angle between L_1 and any line of the fan, and thus varying from 0° to α; this leads to the equation inside the bivariate plot, where L_m is the mean length of the array of lines.

L_m can be obtained by tracing lines at a constant step of either an α or D subdivision. Both possibilities are equally suitable, and we have no specific reason for choosing the first. Let τ be the angle at α from L_1 to L_i, so that $L(\tau) = L_i$ and $\tau = \alpha_i/n$ (Text-fig. 3B). Then:

$$L_m = \frac{1}{\alpha}\int_0^{\alpha} L(\tau)\, d\tau \tag{1}$$

Additionally, by applying the sine rule to Text-figure 3B,

$$L(\tau) = L_1 \frac{\sin\beta}{\sin(\tau+\beta)} \tag{2}$$

so that,

$$L_m = \frac{1}{\alpha}\int_0^{\alpha} L_1 \frac{\sin\beta}{\sin(\tau+\beta)}\, d\tau \tag{3}$$

the solution of which gives:

$$L_m = L_1 \frac{\sin\beta}{2\alpha} \ln\left[\frac{(1+\cos\beta)(1+\cos\gamma)}{(1-\cos\beta)(1-\cos\gamma)}\right] \tag{4}$$

where α is in radians.

From here:

$$L_1 = L_m \frac{2\alpha}{\sin\beta \ln\left[\frac{(1+\cos\beta)(1+\cos\gamma)}{(1-\cos\beta)(1-\cos\gamma)}\right]} \tag{5}$$

Turning again to the triangle D, L_1, L_2, we may also state:

$$D = L_1 \frac{\sin \alpha}{\sin \gamma} \tag{6}$$

so that, finally:

$$D = L_m \frac{2\alpha \sin \alpha}{\sin \beta \sin \gamma \ln \left[\frac{(1+\cos \beta)(1+\cos \gamma)}{(1-\cos \beta)(1-\cos \gamma)} \right]} \tag{7}$$

Now we may easily find the derivative dD/dL_m, here termed S':

$$S' = \frac{dD}{dL_m} = \frac{2\alpha \sin \alpha}{\sin \beta \sin \gamma \ln \left[\frac{(1+\cos \beta)(1+\cos \gamma)}{(1-\cos \beta)(1-\cos \gamma)} \right]} \tag{8}$$

Measurement in actual shells

In consideration of the instrumental problems involved in directly determining tangents to the spiral ribs at apertural points, an indirect procedure has been tested. When observing actual shells one immediately realizes that a quadrangular arrangement arises by taking two pairs of homologous points between two consecutive temporary apertures (either growth lines or other growth-conformable radial ornaments). In this way the triangle corresponding to each D can be reconstructed from five measurements (a, b, c, d, e; see Text-fig. 1) in each quadrangle or cell formed by the crossing of two pairs of longitudinal and radial ornamental elements.

Applying the cosine rule to Text-figure 1,

$$\cos \beta = \frac{a^2+d^2-e^2}{2da}, \quad \cos \gamma_1 = \frac{c^2+e^2-b^2}{2ce}, \quad \cos \gamma_2 = \frac{a^2+e^2-d^2}{2ae},$$

and

$$D = a, \quad \gamma = \gamma_1 + \gamma_2, \quad \alpha = 180° - (\beta + \gamma)$$

The values of σ, β and γ can then be substituted in (8). Note that the five measurements actually define a quadrilateral in three dimensions, which we consider planar by projecting it qualitatively onto the focal plane. In this way S' is not the expansion rate of the adoral rib segment (a), but rather of a segment intermediate between a and b. This procedure can be used with only those shells in which there are aperture-conformable ornaments.

Standardized sectorial-expansion rate S

In brief, S' (see equation [8]) provides the rate at which a given D expands as L_m enlarges. In its present form S' depends monotonically on the measured distance D. For sectors of different D to be compared S' must be standardized. This problem can be tackled by considering that different S' values would be comparable if the respective D lengths were the result of expanding identical initial lengths. S' is thus divided by the original length of the sector chord, namely the length b of the first quadrangle considered, in an apex-to-aperture direction (here named b_I). This procedure only allows a comparison of sectors within the same shell, provided that every b_I is measured at the same growth stage (along the same growth line or radial rib). S'/b_I allows comparison neither of different growth stages on a single shell (provided that a different b_I is used) nor of different specimens. Thus we must standardize b_I itself in order to specify its relative size. The best alternative seems to be to divide b_I by the total initial apertural length (b_{IT}) at the stage where b_I was measured. Thus,

$$S = S' \frac{b_{IT}}{b_I} \tag{9}$$

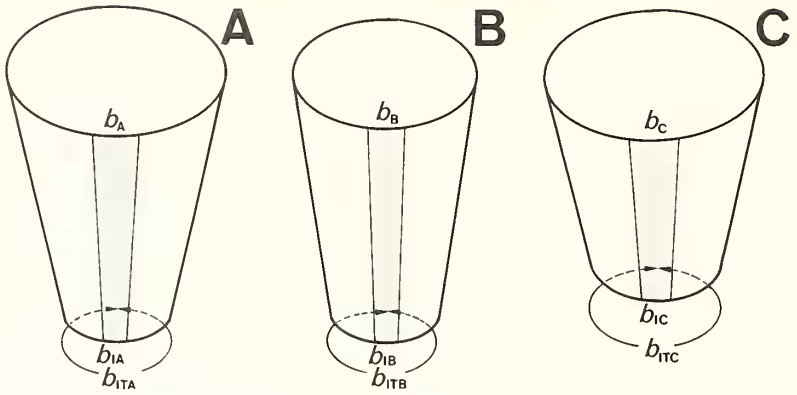

TEXT-FIG. 4. Relation between overall expansion rate (given by the apical angle) and sectorial-expansion rate (S) in three isometric orthoconic shells. A and C expand at the same rate, and faster than B. Correspondingly $S_A = S_C > S_B$.

This can be better understood with an example of orthoconic shells with different overall expansion rates. For the isometric shells of Text-figure 4:

$$L_{mA} = L_{mC} < L_{mB}, \quad b_A = b_C > b_B, \quad b_{IA} = b_{IB} < b_{IC}, \quad b_{ITA} = b_{ITB} < b_{ITC},$$

then:

$$S_A = S_C > S_B,$$

as is apparent from the three cases illustrated.

Text-figure 5 displays the values of S on a plot of α against $\beta-\gamma$, for a fixed value of b_{IT}/b_I. As can be seen, the surface obtained is a slope which is highest at that vertex of the horizontal plane at which α approaches 180° and $\beta-\gamma$ tends to 0°, and descends towards the axis of $\alpha = 0°$. In brief, S increases with α and, for a given α value, with the extreme values of $\beta-\gamma$ (0° or $180°-\alpha$). Text-figure 5 does not display negative values of S. These are obtained when $\alpha > 180°$, in which case α is located past the aperture (D) onwards in the direction of growth. S is not shown near where $\alpha = 180°$ and $\beta-\gamma = 180°$, since these yield infinite S values. The flat left half of the plot denotes a field of impossible values, inside which $\alpha+\beta+\gamma > 180°$.

Finally, one could question whether the actual length (i.e. along the margin) instead of the sector chord length (D) should be considered. There are no simple formulae of the above type for the marginal length, and large deviations may be expected, due both to the value of this length (always greater or, exceptionally, equal to D) and to that of the corresponding mean spiral length (greater than L_m if the aperture is projected, and lesser if invaginated). For similar reasons, S is less representative of the arc expansion when both the relative magnitude of D (compared to the total apertural length) and the complexity of the aperture (presence of projections and invaginations) increase. Teratological deviations of the ornament (e.g. as a result of injuries) may also lead to disruptive results.

Corrected sectorial-expansion rate S_c

The condition of isometry for coiled shells implies that the sectorial-expansion rates are constant around the whorl cross-section or aperture, provided that they are calculated against the revolution angle (see Checa 1991); in contrast, S is the relation D *versus* one linear length (L_m). Since in an ideally isometric shell L_m is a measure of the spiral length, L_m will increase with the distance to the axis of coiling and to the apex for a given growth stage (see Checa and Padilla 1990); therefore S will decrease abaxially and towards the columella in gastropods. Therefore, for comparative purposes, a correction factor for differences in the spiral length must be introduced.

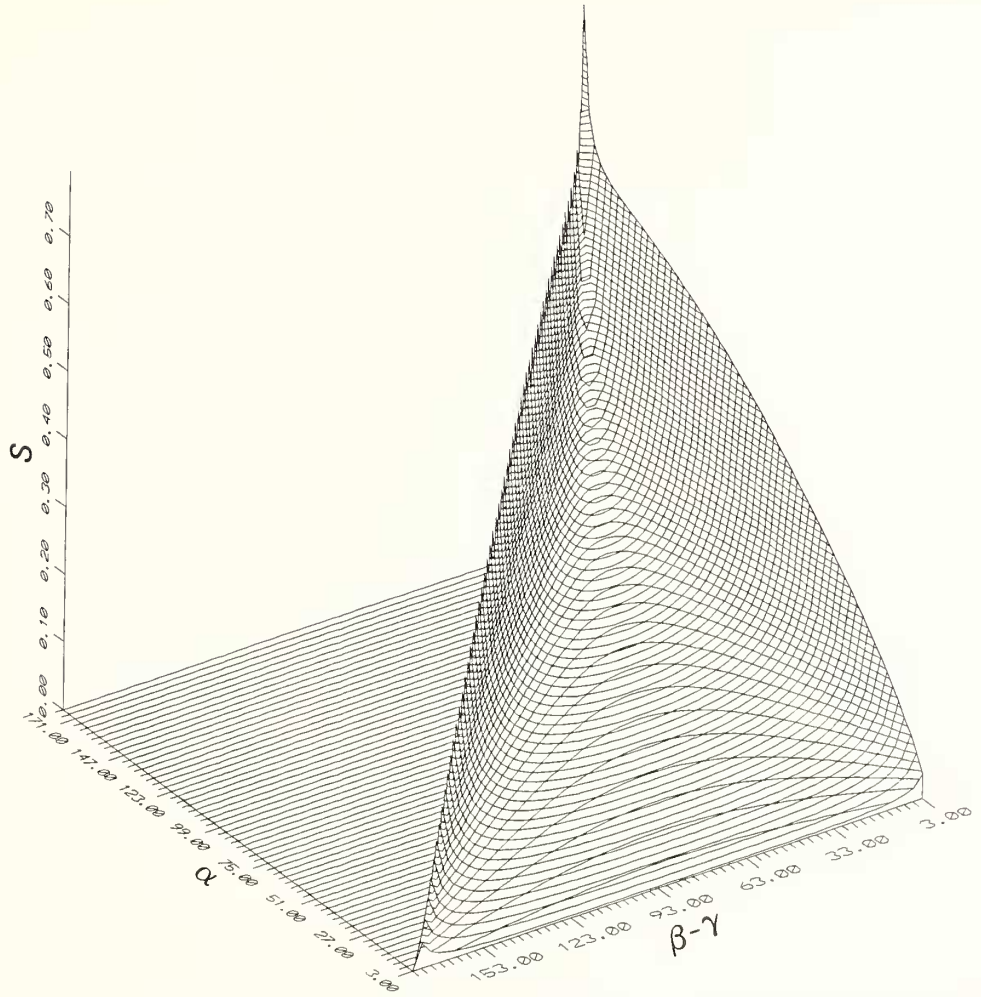

TEXT-FIG. 5. Surface obtained by plotting the values of S between $3° < \alpha < 177°$ and $3° < \beta - \gamma < 177°$, for a constant value $b_1/b_{1T} = 0{\cdot}05$. The side facing the reader should be seen as concave.

Given the measurement procedure described above we will correct according to the relative length of longitudinal ribs for each growth increment (i.e. the cell's longitudinal distance). Since a and b of each cell are limited by common sides (L_1 and L_2; see Text-figure 1) we can define, besides L_m, another l_m between b, l_1 and l_2:

$$l_m = l_1 \frac{\sin\beta'}{2\alpha} \ln\left[\frac{(1+\cos\beta')(1+\cos\gamma')}{(1-\cos\beta')(1-\cos\gamma')}\right] \tag{10}$$

where β', γ' and l_1 can easily be calculated as

$$\sin\gamma' = \frac{e}{b}\sin\gamma_1, \quad \beta' = 180° - (\alpha+\gamma'), \quad l_1 = b\frac{\sin\gamma'}{\sin\alpha}.$$

As the absolute length increment of each cell after an aperture motion between two consecutive

radial ribs we will take $L_m - l_m$. The relative length increment at the ith cell can be obtained by dividing the absolute increment by the mean value of the many $L_m - l_m$ of the same column:

$$M_i = \frac{n(L_m - l_m)_i}{\sum_{i=1}^{n} (L_m - l_m)_i}, \tag{11}$$

where n is the number of cells per column.

Finally, S can be recalculated as

$$S_c = S_i M_i. \tag{12}$$

It must be emphasized that this correction method can only be applied if the relative apertural orientation between consecutive apertures remains more or less the same (as in *Distorsio*). Otherwise, $L_m - l_m$ will additionally decrease towards the intersection of the aperture planes, since a approaches b gradually. When apertural orientation and/or shape change ontogenetically special procedures must be implemented.

SECTORIAL-EXPANSION ANALYSIS OF *DISTORSIO*

The morphology and adaptive significance of *Distorsio* has been analysed and discussed at length by Linsley (1977), Linsley and Javidpour (1980), Stanley (1988) and Ackerly (1989*b*). We have chosen this gastropod because it displays a highly distorted morphology due to the periodic inflation and deflation of the spiral tube (usually every two-thirds of a whorl). Given its complexity this morphology can hardly be the subject of traditional morphometric analyses.

Material and measurement technique

We have systematically measured three specimens of *Distorsio reticulata* Röding, although complementary observations were made on another three specimens of the same species and two of *D. anus* (Lamarck). All this material is Recent, from the East Pacific (Philippines), and is presently housed at the Department of Stratigraphy and Palaeontology of the University of Granada (abbreviated PUG) and the National Museum of Natural Sciences, Madrid (MNCN). *D. reticulata* bears a typically reticulated ornamentation (Text-fig. 6) formed by the crossing of radial (parallel to the aperture) and longitudinal ribs. Small knobs form at the intersection of two ribs. The determination and tracing of homologous points is much eased by the existence of longitudinal lines with slightly positive relief which occur superimposed onto the main ornament. In well-preserved specimens they coincide with brown colour lines and seem to be sites of emergence of periostracal hairs.

From our three specimens we have analysed only the last growth episode (between the ultimate and penultimate constrictions). For an easy identification of ornamental cells of the grid, a matrix labelling has been used. In this way, 17–18 (depending on the specimen) longitudinal rows by 16–19 radial columns of cells have been distinguished (see Text-figs 6–7). Further towards the siphonal canal the great relative width of spiral ribs does not allow enough precision. Given the close morphological similarity between the three specimens, rows represent approximately homologous shell portions in each of them. All cells are formed by first-order ribs, except for those bounding rows 2–3 and 5–6.

Each cell of the reticulum was drawn with a Wild camera lucida M8 at 25-fold magnification, the shell being continuously reorientated so that each quadrangle was qualitatively considered to lie parallel to the stage. Since quadrangles are actually three-dimensional, an approximation is made in this respect. The five measurements for each cell (see above) were then taken with a 0·5-mm graded ruler. To test the accuracy of this procedure, we remeasured specimen PUG.G.12 with a Wild binocular microscope M7S, attached to a Sony Magnescale unit for measuring stage displacement (precision = 1 μm). Both kinds of values were only exceptionally found to differ by

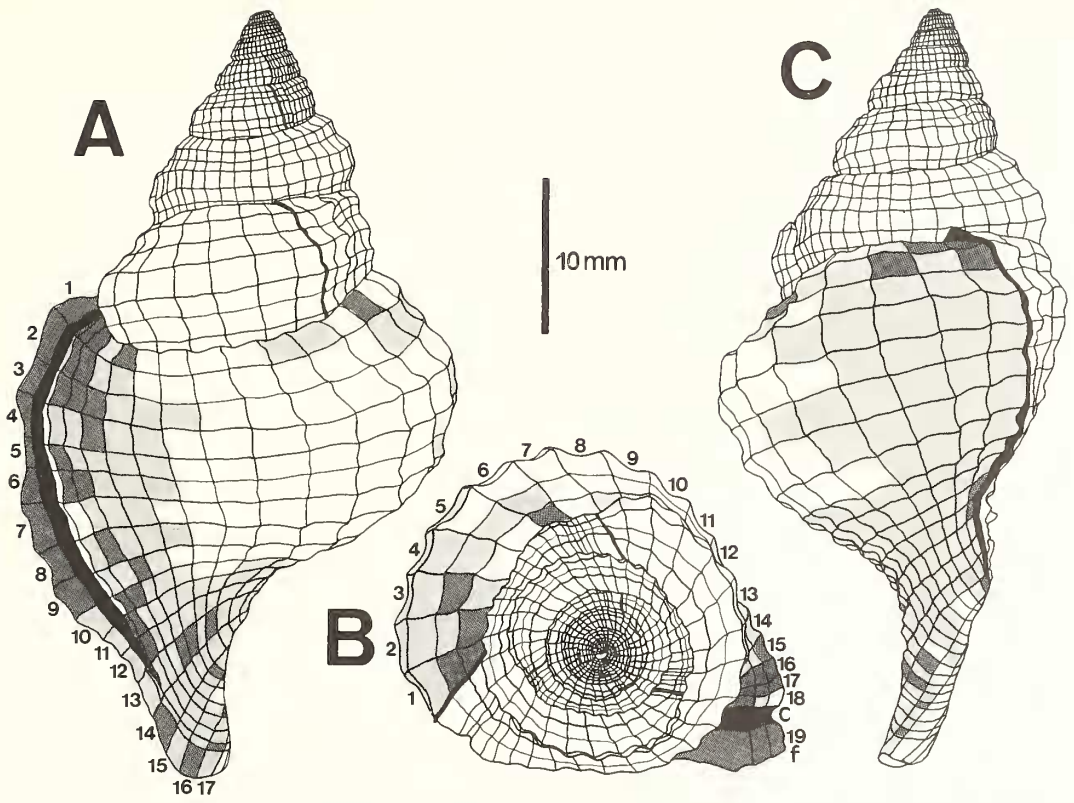

TEXT-FIG. 6. A–C, Schematic morphology of *Distorsio reticulata* Röding (PUG.G.12; same specimen as in Checa 1991, fig. 4). Lateral (A, C) and apical (B) views; numbers on A and B refer, respectively, to the 17 rows by 19 columns of reticular cells distinguished; white cells have yielded $S_c < 0$, medium grey cells $0 < S_c < 2$ and dark cells $S_c > 2$ (compare with Text-fig. 7A). Abbreviations: c, constriction; f, flaring. Camera lucida drawings.

more than 15 per cent, the major differences being found close to the siphonal canal, probably owing to the diffuse nature of ribs at this zone. The values for b_1 were taken at column 1. In all, 5655 measurements were taken, the mathematical processing of which was performed by a short computer program, written in TURBO PASCAL for an IBM PC, which is available on request from the authors.

Discussion and constructional interpretation

The sectorial-expansion maps are displayed in Text-figure 7. They have been obtained by plotting curves of equal S_c values on a row-column diagram. Curves have been smoothed by cubic splines (tension factor = 0·5). Commercial software has been used for the representation.

A marked similarity exists between the three maps, so that a common morphogenetic pattern can be inferred. From a constructional point of view, the following phases can be differentiated from the penultimate towards the last varix.

1. The growth period begins with a fast-expansion phase which occupies some 3 to 4 columns.

2. This expansion decelerates gradually to give way to a contraction phase affecting 8 to 9 columns in the shell half close to the adapical suture and centred in the growth episode; abapically this phase narrows at mid-shell in MNCN.P-M.4.317*b* (Text-fig. 7C) or becomes interrupted in

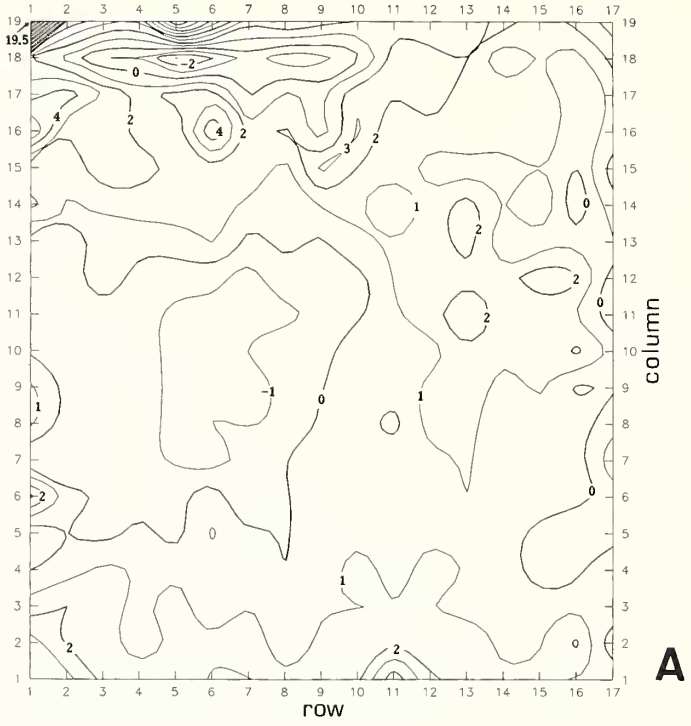

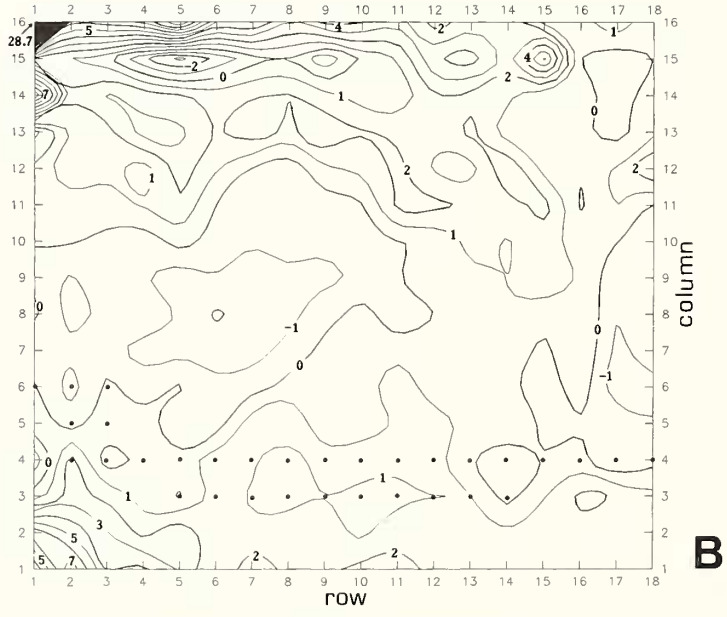

TEXT-FIG. 7A–B. For legend see opposite.

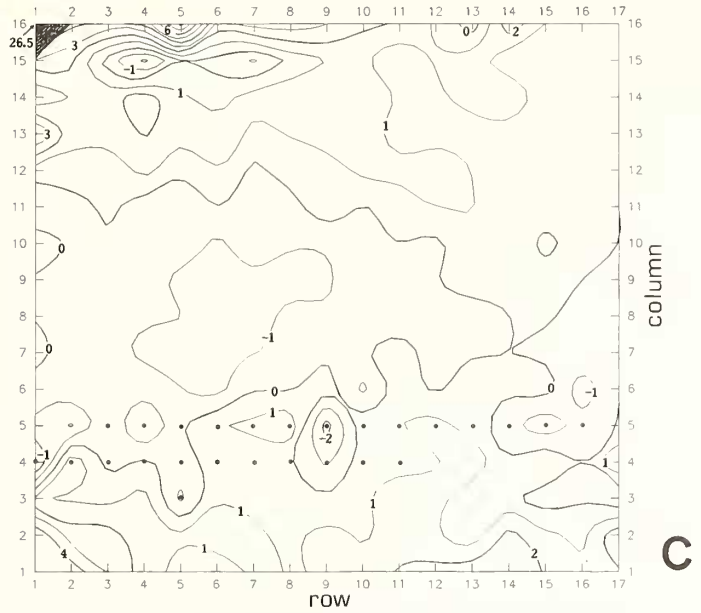

TEXT-FIG. 7. Sectorial-expansion (S_c) maps for the last growth episode of three specimens of *Distorsio reticulata* Röding. A, specimen PUG.G.12; same specimen and cell numbering as in Text-figure 6. B–C, specimens MNCN.P-M.4.317*a* (B) and MNCN.P-M.4.317*b* (C). Dots mark sectors affected by predatory shell breakage.

PUG.G.12 and MNCN.P-M.4.317*a* (Text-fig. 7A–B) to spread or reappear close to the siphonal canal.

3. Farther towards the aperture another narrow expansion phase (3 to 4 columns) takes place, which does not reach the siphonal canal.

4. A narrow, elongate depression is placed at the penultimate column, and never surpasses row 11 or 12.

5. The last column displays very high S_c values (especially the peak at row 1), which lessen once more abapically along the column.

Phases 1 and 2 correlate well to the bulging and deflation stages of the spiral tube (and, by extension, of the soft body) during the growth episode (compare Text-figs 6, 7A). It is thus evident that alternate periods of fast expansion and low expansion or contraction of discrete sectors of the aperture during growth cause the distorted coiling typical of *Distorsio*, no additional considerations being needed. This differs from Linsley and Javidpour's (1980) and, particularly, Ackerly's (1989*b*) conclusion, in his analysis by stereographic projection, that there is a cyclic shift in the orientation of the coiling axis. Even though this process would also imply sectorial-expansions, these would presumably take place exclusively both at the adapical sutures and near the siphonal canal, but will never yield the above complex pattern. Phase 4 coincides in all cases with the pre-apertural constriction (which extends up to row 11 in PUG.G.12, or 12 in MNCN.P-M.4.317*a–b*), which is, no doubt, caused by a sudden contraction of the soft body. Phase 5, on the other hand, implies a bursting expansion leading to the apertural flaring.

Some irregularities are worth mentioning. The one along the most adapical row (number 1) can be attributed to its adaptation to the ornamentation of the previous whorl. Additionally, predatory shell breakage (see below) induces other irregular fields in Text-figure 7B and, especially, 7C (sectors affected are indicated by dots).

All these features fit well within the view of the mantle as a pneu, that is, an elastic membrane,

the shape of which is maintained by internal hydrostatic pressure (see Savazzi 1990). Nevertheless, there seem to be differences between different parts of the aperture. We should remember that all phases are interrupted or lessened at about the eleventh or twelfth row (this being also the abapical limit for constrictional invaginations). In our specimens this strip is a bending zone of the shell marking the limit between the columellar and the remaining convex part of the aperture. The latter is the only one which seems to be able to inflate and deflate periodically to a great extent, thus displaying an apparently pneumatic behaviour. The columellar part of the aperture imitates this behaviour, but to a much lesser degree. This feature would imply that *Distorsio*'s apertural mantle either behaves as a double-pneu (see Savazzi 1990, p. 205) or as a single-pneu with different expansion capabilities throughout. To decide between these alternatives, further studies on the mechanical properties of the mantle are necessary.

Functional considerations

Linsley (1977) argued that distortion from normal helical growth allows *Distorsio* to protect the aperture by maintaining it in a plane tangential to the preceding whorl and parallel to the axis of coiling. However, neither is the aperture parallel to the coiling axis in *D. reticulata* (they meet at 10° to 12°), although it is in *D. anus*, nor is distortion strictly necessary for this purpose (in fact other cymatiids manage without distortion). Therefore this functional hypothesis seems rather weak.

Coincidentally, the three specimens of *D. reticulata* labelled MNCM displayed very conspicuous predatory features, indicating that the gastropod survived peeling back of the shell of at least between one-fourth and one-thirteenth of a revolution. The limit of peeling is always close to the penultimate varix. Although our statistics are not significant, this kind of predation may be frequent in this genus and the soft body must have been able to retract deeply within the shell (in much the same way as in high-spired, many-whorled turritelliform gastropods). We suggest here that the periodic bulgings of the spiral may partly account for this ability by providing extra room for the body when retraction takes place.

Further, it is evident from the apical view (see Text-fig. 6B) that distortion shifts the shell's centre of gravity towards the substrate and closer to the coiling axis, compared to normal coiling. This accounts for a greater stability, which is enhanced by increasing the lever arm of the shell through apertural expansions and columellar calluses (which in *D. anus* may encircle the whole aperture).

Finally, the alternation of constrictional invagination and apertural flaring corrugates and thus might strengthen the final aperture of each growth episode.

GENERAL CONCLUSIONS

The present sectorial-expansion rate S_e can be considered as a morphometric methodology which enables us to quantify local changes in shape along the biological generating curve (aperture). Although the mode of coiling cannot be unequivocally described in this way, we are dealing with a high-resolution tool which is useful in morphological and morphogenetic studies. The potential applications of this methodology are many. Since the sectorial-expansion maps depicted above may in fact be regarded as aperture-behaviour maps, they allow us to discern the constructional basis (expansion of the aperture versus change in the coiling programme; see Checa 1991) of a given ontogenetic change. Although we have been dealing here with shells, we should stress that parts of them (e.g. individual ornaments) or other taxa (e.g. polychaete jaws, mammal teeth) are potential subjects of study for modified versions of S_e, provided that an ontogenetic record exists and that trajectories of homologous points are traceable. Finally, the time-consuming nature of this method must not prevent it from being employed as an additional criterion in systematic studies.

Acknowledgements. This paper is affectionately dedicated to Dr A. Linares, who was the Head of this Department for nineteen years from its foundation in 1967. We are also indebted to Dr J. Martínez Aroza (Department of Applied Mathematics, University of Granada) and Dr A. Padilla (Department of Geodynamics, University of Granada) for technical assistance, and Mr O. Soriano (National Museum of

Natural Sciences, Madrid) for providing specimens. Special thanks are given to Dr J. M. C. Hutchinson (School of Mathematics, University of Bristol) who improved this paper substantially, far beyond his duties as a reviewer. Dr M. de Renzi (Department of Geology, University of Valencia) critically read an initial version. The present study has been financed by the Research Project PB.0887 (CICYT) and the EMMI Research Group (JA).

REFERENCES

ACKERLY, S. C. 1989*a*. Kinematics of accretionary shell growth, with examples from brachiopods and molluscs. *Paleobiology*, **15**, 147–164.

—— 1989*b*. Shell coiling in gastropods: analysis by stereographic projection. *Palaois*, **4**, 374–378.

CHECA, A. 1991. Sectorial expansion and shell morphogenesis in molluscs. *Lethaia*, **24**, 97–114.

—— and PADILLA, A. 1990. Length versus revolution angle in coiled shells. *Lethaia*, **23**, 310.

ILLERT, C. 1989. Formulation and solution of the classical seashell problem. II. Tubular three-dimensional seashell surfaces. *Il Nuovo Cimento*, **11D**, 761–780.

LINSLEY, R. M. 1977. Some 'laws' of gastropod shell form. *Paleobiology*, **3**, 196–206.

—— and JAVIDPOUR, M. 1980. Episodic growth in Gastropoda. *Malacologia*, **20**, 153–160.

McGHEE, G. R. 1978. Analysis of the shell torsion phenomenon on the Bivalvia. *Lethaia*, **11**, 315–329.

—— 1980*a*. Shell form in the biconvex articulate Brachiopoda: a geometric analysis. *Paleobiology*, **6**, 57–76.

—— 1980*b*. Shell geometry and stability strategies in the biconvex Brachiopoda. *Neues Jahrbuch für Geologie und Paläontologie, Monatshefte*, **1980** (3), 155–184.

MEINHARDT, H. 1984. Models for positional signalling, the threefold subdivision of segments and the pigmentation pattern of molluscs. *Journal of Embryology and Experimental Morphology* (Supplement), **83**, 289–311.

—— and KLINGER, M. 1987. A model for pattern formation on the shells of molluscs. *Journal of Theoretical Biology*, **126**, 63–89.

OKAMOTO, T. 1988*a*. Analysis of heteromorph ammonoids by differential geometry. *Palaeontology*, **31**, 35–52.

—— 1988*b*. Changes in life orientation during the ontogeny of some heteromorph ammonoids. *Palaeontology*, **31**, 281–294.

—— 1988*c*. Developmental regulation and morphological saltation in the heteromorph ammonite *Nipponites*. *Paleobiology*, **14**, 272–286.

RAUP, D. M. 1961. The geometry of coiling in gastropods. *Proceedings of the National Academy of Sciences*, **47**, 602–609.

—— 1962. Computer as aid in describing form in gastropod shells. *Science*, **138**, 150–152.

—— 1966. Geometric analysis of shell coiling: general problems. *Journal of Paleontology*, **40**, 1178–1190.

—— 1967. Geometric analysis of shell coiling: coiling in ammonoids. *Journal of Paleontology*, **41**, 43–65.

—— and MICHELSON, A. 1965. Theoretical morphology of the coiled shell. *Science*, **147**, 1294–1295.

SAVAZZI, E. 1985*a*. SHELLGEN, a BASIC program for the modeling of molluscan shell ontogeny and morphogenesis. *Computer and Geosciences*, **11**, 521–530.

—— 1985*b*. Adaptive themes in cardiid bivalves. *Neues Jahrbuch für Geologie und Paläontologie, Abhandlungen*, **170**, 291–321.

—— 1987. Geometric and functional constraints on bivalve shell morphology. *Lethaia*, **20**, 293–306.

—— 1990. Biological aspects of theoretical shell morphology. *Lethaia*, **23**, 195–212.

SEED, R. 1980. Shell growth and form in the Bivalvia. 23–67. *In* RHOADS, D. C. and LUTZ, R. A. (eds). *Skeletal growth of aquatic organisms. Biological records of environmental change*. Plenum Press, New York and London, xiv + 750 pp.

STANLEY, S. M. 1988. Adaptive morphology of the shell in bivalves and gastropods. 105–141. *In* TRUEMAN, E. R. and CLARKE, M. R. (eds). *The Mollusca*, Volume 11. *Form and function*. Academic Press, San Diego, xxviii + 504 pp.

ANTONIO CHECA
Departamento de Estratigrafía y Paleontología
Facultad de Ciencias
Universidad de Granada
18071-Granada, Spain

ROQUE AGUADO
Departamento de Estratigrafía y Paleontología
E.U. Politécnica de Linares
Universidad de Granada
23700-Linares, Spain

Typescript received 6 January 1992
Revised typescript received 10 March 1992